The ISME Journal (2014) 8, 804–815

www.nature.com/ismej

ORIGINAL ARTICLE

Ecological succession among iron-oxidizing bacteria

Emily J Fleming[1], Ivona Cetinić[2], Clara S Chan[3], D Whitney King[4] and David Emerson[1]
[1]*Bigelow Laboratory for Ocean Sciences, East Boothbay, ME, USA;* [2]*University of Maine, Darling Marine Center, Walpole, ME, USA;* [3]*Department of Geological Sciences, University of Delaware, Newark, DE, USA and* [4]*Department of Chemistry, Colby College, Waterville, ME, USA*

Despite over 125 years of study, the factors that dictate species dominance in neutrophilic iron-oxidizing bacterial (FeOB) communities remain unknown. In a freshwater wetland, we documented a clear ecological succession coupled with niche separation between the helical stalk-forming Gallionellales (for example, *Gallionella ferruginea)* and tubular sheath-forming *Leptothrix ochracea*. Changes in the iron-seep community were documented using microscopy and cultivation-independent methods. Quantification of Fe-oxyhydroxide morphotypes by light microscopy was coupled with species-specific fluorescent *in situ* hybridization (FISH) probes using a protocol that minimized background fluorescence caused by the Fe-oxyhydroxides. Together with scanning electron microscopy, these techniques all indicated that Gallionellales dominated during early spring, with *L. ochracea* becoming more abundant for the remainder of the year. Analysis of tagged pyrosequencing reads of the small subunit ribosomal RNA gene (SSU rRNA) collected during seasonal progression supported a clear Gallionellales to *L. ochracea* transition, and community structure grouped according to observed dominant FeOB forms. Axis of redundancy analysis of physicochemical parameters collected from iron mats during the season, plotted with FeOB abundance, corroborated several field and microscopy-based observations and uncovered several unanticipated relationships. On the basis of these relationships, we conclude that the ecological niche of the stalk-forming Gallionellales is in waters with low organic carbon and steep redoxclines, and the sheath-forming *L. ochracea* is abundant in waters that contain high concentrations of complex organic carbon, high Fe and Mn content and gentle redoxclines. Finally, these findings identify a largely unexplored relationship between FeOB and organic carbon.
The ISME Journal (2014) **8,** 804–815; doi:10.1038/ismej.2013.197; published online 14 November 2013
Subject Category: Microbial population and community ecology
Keywords: FeOB; *Gallionella*; *Leptothrix ochracea*; neutrophilic; freshwater iron mats; *Sideroxydans*; seasonal dynamics

Introduction

Bacterial succession has been a difficult process to study in the field largely because of the lack of easily identifiable, distinct species markers. Iron-oxidizing bacteria (FeOB) are unusual in that they generate large quantities of morphologically distinct, biogenically formed iron oxyhydroxide structures, or morphotypes, that can be easily recognized by light microscopy (van Veen *et al.*, 1978; Winogradsky, 1888; Emerson *et al.*, 2010; Chan *et al.*, 2011). Different morphotypes have been linked phylogenetically, through cultivation-independent studies, to the order Gallionellales (stalk and particulates) or the genus *Leptothrix* (sheaths; including the dominant sheath-forming FeOB, *L. ochracea)* (Chan *et al.*, 2011; Fleming *et al.*, 2011). In slow-moving waters, these FeOB produce loosely flocculent oxyhydroxide layers that can be centimeters thick, whereas in faster-flowing waters the oxyhydroxides form thinner, denser layers of only a few millimeters. These microbial iron mats are hotspots of microbial activity that entrain nutrients and trace metals. From a practical standpoint, the activity of FeOB leads to biofouling and deterioration of wells, pipes and water distribution systems (Katsoyiannis and Zouboulis, 2006; Emerson *et al.*, 2010; Li *et al.*, 2010); thus, there is interest in determining the cause of their proliferation.

Climatic and environmental factors contribute to microbial community dynamics and variance (Kent *et al.*, 2007). FeOB communities are typically constrained to redoxcline habitats with high concentrations (10s–100s of μM) of Fe(II). The physical or chemical niche preference of the two most apparent FeOB, however, has been

Correspondence: EJ Fleming, Bigelow Laboratory for Ocean Sciences, PO Box 380, East Boothbay, ME 04544, USA.
E-mail: efleming@bigelow.org
Received 21 June 2013; revised 2 September 2013; accepted 22 September 2013; published online 14 November 2013

difficult to determine. It has been challenging to find locations where one FeOB morphotype (that is, sheaths or stalks) and the small subunit ribosomal RNA (SSU rRNA) gene sequences clearly dominate over the other (for example, Haaijer *et al.*, 2008; Duckworth *et al.*, 2009; Bruun *et al.*, 2010; Gault *et al.*, 2012). One explanation for this may be that localized gradients within an ecosystem result in microenvironments that allow for different FeOB to coexist. An example of this was seen in a highly structured iron mat in Denmark in which *L. ochracea* dominated most of the mat, but there were still small areas where the stalks of *Gallionella* were prevalent, even within a few centimeters of *L. ochracea*-dominated regions (Emerson and Revsbech, 1994). The first systematic study that shed light on the population dynamics of FeOB in multiple iron mat communities was performed in Wisconsin and Minnesota by Harder (1919). He observed that some Fe-rich springs and Fe-rich accretions in underground mine shafts were dominated by stalk formers, whereas other wetland-associated sites were dominated by *L. ochracea*-like sheaths. Harder hypothesized that the heterogenous distribution of different FeOB forms was due to differences in the chemical composition of waters feeding the iron mats; however, verification of this hypothesis and specification of key parameters have been elusive until now.

On observing samples collected from a local iron mat community, initially by light microscopy, we identified a temporal variation in the FeOB populations of a freshwater stream. It appeared to be dominated by *Gallionella*-like stalks in the spring and by *Leptothrix*-like sheaths in the summer. On the basis of these preliminary observations, we hypothesized that there is a distinct successional transition between dominant FeOB morphotypes, and that the chemical composition of the waters is likely responsible for this pattern. Defining these temporal dynamics allowed us to better understand the ecological niches occupied by different FeOB communities and predict which resources favor different populations of FeOB that are associated with different morphotypes.

Materials and methods

Site and sample collection

Freshwater iron mats associated with a small first-order stream in Boothbay Harbor, ME, adjacent to Lakeside Drive (LD; Figure 1; 43°51.6999′N, 69°38.9299′W), were observed during five seasons (2008–2012) and regularly sampled during the 2009 and 2010 seasons. The general site characteristics were described in Fleming *et al.* (2011) and additional details are provided in Supplementary File 1. Depending on the morphological structures present in the mats, the mats and the water above the mat were sampled at either weekly or monthly intervals for analysis of biological, chemical and physical parameters.

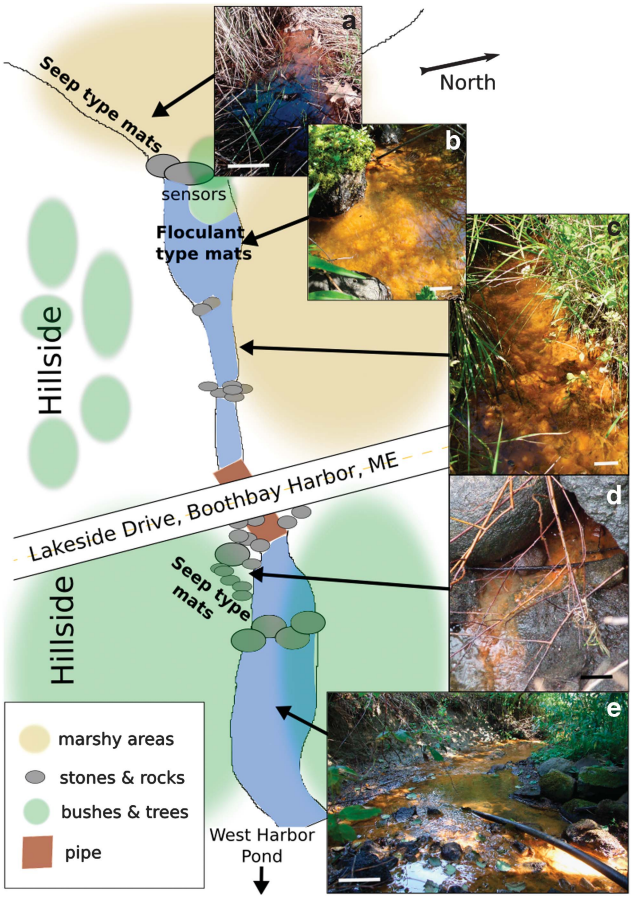

Figure 1. Lakeside Drive study site in the town of Boothbay Harbor, Maine. The length of stream and marshy areas is approximately 75 m. The study site includes several mat types: seep type mats (**a, d**) in the early spring and flocculent type mats (**b**, **c, e**) in the late spring/early summer. Scale bars are 10 cm (images **a–d**) and 100 cm (image **e**). Images (**a–d**) were taken facing upstream, and image (**e**) was taken facing downstream.

Mats were sampled using a Pasteur pipette to collect only the top 0.5 cm that composed the outer layer of either loosely flocculent or condensed mats. This outer section is the most active accreting region, and has been shown to contain a high proportion of FeOB (Emerson and Weiss, 2004; Fleming *et al.*, 2011).

Microscopy and structural analysis of mat community

For structural analysis by light microscopy or scanning electron microscopy (SEM), fresh samples were preserved by adding glutaraldehyde (2.0% final concentration; Electron Microscopy Sciences, Hatfield, PA, USA) and stored at 4 °C until analysis. The percentage of biogenic Fe-oxyhydroxide structure (stalk, sheath or particulate) in each sample was determined by first spreading 10 µl of sample on an agarose-coated slide (Electron Microscopy Sciences) and then capturing at least

10 fields of view with 15 structures (on average) present in each microscopic field. Microscopic analysis was performed using an Olympus BX60 microscope equipped with a QICAM FAST CCD camera and QCapture Pro software (QImaging, Surrey, BC, Canada) as described in Emerson and Moyer (2002). Images were then imported into ImageJ (Rasband, 2004), and each structure was outlined using a Wacom Intuos4 Pen tablet (Vancouver, WA, USA). The surface area of each outlined structure was calculated using the area analysis tool in ImageJ, and counted toward the total percentage area for each structure type. In the fall after the summer transition, sheaths were predominant, and the sheath and stalk ratio was evaluated qualitatively by microscopy.

SEM and EDX analysis

Samples for SEM were dehydrated in an ethanol series and critical point dried (Autosamdri-815B CPD), mounted on an aluminum stub and coated with carbon (Denton Bench Top Turbo III coater). Imaging was performed at the Delaware Biotechnology Institute Bioimaging Facility using a Hitachi S-4700 field emission SEM with an accelerating voltage of 3.0 kV. Energy dispersive X-ray (EDX) spectroscopy was performed at 15 kV using an Oxford Inca X-act detector.

Fluorescent In Situ Hybridization

For fluorescent *in situ* hybridization (FISH), freshly collected mat was preserved in 4% paraformaldehyde for 1.5 h, washed three times with 1× phosphate-buffered saline, resuspended in 1:1 phosphate-buffered saline/ethanol solution and stored at −20 °C. A known sample volume (between 3 and 20 μl) was spread into a ClearCell slide (Thermoscientific, Cell Line Brand, Portsmouth, NH, USA) and air-dried at room temperature.

Several potential Gallionellales-specific probe sequences were designed using ARB software (Ludwig *et al.*, 2004) in combination with the Silva 102 database (Pruesse *et al.*, 2007). Probes were designed to incorporate members of the Gallionellales order including *Gallionella* and *Sideroxydans*. Probe Gal221 (5′-CTTTCGGAGTGGCCGAT-3′; (Eurofins MWG Operon, Huntsville, Alabama, USA)) was ranked highly by the probe match tool in ARB and further tested for its ability to hybridize to cells.

Cy3-labeled candidate probe Gal221 was then evaluated at various stringencies by its ability to hybridize with *Sideroxydans lithitrophicus* ES-1 and iron mats enriched in *Gallionella* stalks. Probe stringency was modulated by formamide concentration using the standard FISH protocols in combination with several of the blocking reagents used for CARD (Catalyzed Reporter Deposition)-FISH protocols (Fuchs *et al.*, 2007; Fleming *et al.*, 2011). Probe stringency at different formamide concentrations was determined by measuring relative fluorescence using an epifluoresence microscope as described in Fleming *et al.* (2011). The optimum stringency for Gal221 probe was 35% formamide.

For cell counts, the Gal221 probe, as well as the Lepto175 probe (for *L. ochracea*; ATCCACAGATCA CATGCG; also (Eurofins MWG Operon, Huntsville, Alabama) (Fleming *et al.*, 2011), was used. Each sample analyzed by FISH was probed in triplicate, and at least 10 fields were counted per well. In addition, total microbial cells were counted in triplicate by drying cells on ClearCells slides, staining them with Syto13 (Invitrogen-Life technologies, Grand Island, NY, USA) and counting all the cells (⩾10 fields). Epifluoresence imaging and visualization was performed using an Olympus BX60 microscope.

Community sequencing and data processing

To understand the microbial population structure of the iron mat community, eight temporally spaced samples from LD were analyzed using tagged pyrosequencing. Total community DNA was extracted from ⩾15 ml of freshly collected (not frozen) mat sample using MoBio Power Water DNA extraction (as per the manufacturer's recommendations; Carlsbad, CA, USA) and stored at −20 °C. Extracted DNA samples (at DNA concentrations of 3.4–100 ng μl^{-1}) were sent for tagged pyrosequencing of the V4–V6 region to the Research and Testing Laboratory (Lubbock, TX, USA), and processed as described in Dowd *et al.* (2008). Samples were sequenced on a Roche 454 FLX system with Titanium Chemistry (Roche, Nutley, NJ, USA) using tags, barcodes and primers listed in Supplementary Table 1. Samples were processed in Mothur 1.28.0 according to the Schloss Standard Operating Protocol (Schloss *et al.*, 2011; http://www.mothur.org/wiki/Schloss_SOP, first accessed in March 2012). After a stringent processing protocol that involved trimming, quality checking, removing chimeras and screening using Mothur (Table 1), sequences were aligned using the Silva database (Pruesse *et al.*, 2007) and classified using a modified version of the NCBI classification hierarchy that included several known FeOB as described in McBeth *et al.* (2013).

All sequences from the tagged pyrosequencing libraries were submitted to the NCBI short-read archive under accession number SRP008006.

Analysis of physicochemical constituents

Physicochemical parameters at the LD site were determined both *in situ* and by laboratory analysis of collected samples. Continuous *in situ* water temperature was measured using three Hobo Pendant temperature/light sensors (Onset Computers, UA-002-64, Bourne, MA, USA), and air temperature was obtained from NOAA data for the nearby Wiscasset

Table 1 Statistical summary of tagged pyrosequencing reads for samples used in this study

Date of sample collection	*% of high quality sequences post-processing*	*Number of sequences post-processing*	*Estimated % coverage (0.03)*[a]	*Number of operational taxonomic units (0.03)*[a]	*Berger Parker index (0.01)*[a]	*Inverse simpson index (0.03)*[a]	*% sequences from genus or order*	
							Leptothrix spp.	Gallionellales
LD 4/22	15.1	922	96.10	87	17.35	14	0.5	4.8
LD 5/14	10.5	471	47.13	302	1.91	163	0.0	1.1
LD 5/21	46.2	1590	70.82	684	2.95	156	0.2	0.9
LD 5/23	18.4	976	66.91	417	11.78	32	13.1	1.4
LD 6/01	13.6	811	80.15	261	7.64	56	3.8	0.4
LD 6/04	38.5	2340	79.87	697	7.31	37	7.7	2.9
LD 7/02	17.6	1115	69.51	446	9.24	41	4.2	1.8
LD 9/30	14.9	1104	84.42	246	21.47	11	22.7	1.8

Abbreviation: LD, Lakeside Drive.
[a]Percent similarity clustered.

Airport, ME (http://www.ncdc.noaa.gov/cdo-web/). The stream pH was measured *in situ* with either a Check-Mite pH-20 (Corning, Tewksbury, MA, USA) or color-pHast EMD pH indicator strips (EMD, Gibbstown, NJ, USA). Oxygen profiles were determined in the field in April and October with a Clark-type electrode and an ISO_2-dissolved oxygen meter (World Precision Instruments, Sarasota, FL, USA).

Fe(II) concentrations were determined by ferrozine assay, in which water samples were filtered through a 0.2 μm syringe filter (Millipore, Billerica, MA, USA), added to ferrozine (Stookey, 1970), buffered in acetic acid and reduced with hydroxylamine (total iron only). The sample absorbance (in sextuplicates) was measured on a Thermo Scientific Multiskan MCC plate reader (Rockford, IL, USA) at 562 nm and converted to iron concentrations based on a standard curve of known Fe(II) concentrations.

Water samples for inorganic nutrients analysis were collected with a sterile 35 ml syringe and filtered through a cellulose acetate 0.2-μm filter (VWR, Radnor, PA, USA). Trace metal clean nitric acid (trace metal grade, Sigma; 80 mM final concentration) was added to each sample and stored at 4 °C until analysis by inductively coupled plasma atomic emission spectroscopy (ICP-AES) (Spectro, Arcos, Kleve, Germany). The instrument was calibrated using multi-element standards in the range of 0–10 000 p.p.b. with detection limits of less than 5 p.p.b. for most elements. All samples were run in triplicate (Supplementary File 2).

Water samples for dissolved organic carbon (DOC) and spectral absorption coefficient of the dissolved matter ($a_{diss}(\lambda)$) were filtered in the field through a 0.45 μm nominal pore size Whatman GF/F filter (Whatman, Piscataway, NJ, USA) to remove particulates. The filtrate was stored in RBS 35 Detergent Concentrate (Thermo Scientific, Rockford, IL, USA) washed glass vials, at either −80 °C or −20 °C, until analysis. The DOC samples were analyzed at Horn Point Laboratory, University of Maryland, on Shimadzu TOC-5000A following the method described in Sugimura and Suzuki (1988). The filtered samples collected for determination of a_{diss} (λ) were acclimated to room temperature (~20 °C), transferred to 1-cm light path quartz cuvettes and analyzed on a Varian Cary 50 Bio UV-visible spectrophotometer (Santa Clara, CA, USA) at 1-nm resolution with a wavelength range of 200–800 nm. Each sample was scanned three times. The baseline correction for each spectral scan was carried out using Milli-Q water alone. Instrument stability was monitored throughout the analysis by running Milli-Q water blanks. All water samples were analyzed within 5 months of collection.

Two a_{diss} slope ratios (275–295-nm slope: 350–400-nm slope) can be used to relate changes in dissolved organic matter to DOC molecular weight (MW) (Helms *et al.*, 2008). The increase in these two slope ratios indicates a decrease in MW for freshwater, estuarine and marine samples. Following the approach outlined by Helms *et al.*, (2008), a linear function was fitted on the log-transformed data from two wavelength ranges: 275–295 nm and 350–400 nm. For convenience, here we have used inverted (Helms *et al.*, 2008) slope ratio, slope (350–400 nm)/slope (275–295 nm), wherein an increase in spectral slope indicates an increase in MW and an increase in functional aromaticity.

Statistical analysis

Redundancy analysis (RDA), a multivariate canonical ordination analysis, was used to define the relationships between FeOB species abundances (dependent variables) and environmental parameters (explanatory variables) that were not easily apparent in simple pair-wise analyses. This multivariate statistical analysis facilitates visualization of observed trends by coupling taxonomical and environmental data sets in a single two-dimensional

biplot (Ramette, 2007), providing a more robust interpretation of the data. Prior to the analysis, environmental data were standardized by subtracting the mean and dividing by the standard deviation. The FISH-based cell counts were logarithmically transformed. In the resulting distance biplot, species locations and distances between them (based on the respective ordination scores) indicated their similarity to one another. Environmental parameters are depicted as vectors: the vector length indicates the importance to the ordination (and its effect on species variation); the vector direction depicts the gradient of the respective environmental variable in the ordination space (starting from the center out); both length and direction describe its correlation with the axes. The species (dependent variables) and the environmental vector proximity in the biplot (ordination space) indicate the correlation strength. The environmental variables that had a canonical coefficient lower than 0.05 were omitted from the biplot.

Principal Coordinates Analysis (PCoA) was used to assess the similarity in community structure along the sampling period. Ordination was generated in R (R Core Team (2012), http://www.r-project.org) using a Yue and Clayton-based distance matrix calculated in Mothur from the tagged pyrosequencing data set where relative abundance of operational taxonomic units (OTUs) was defined at 3% OTU definition level.

Results

Repeated seasonal development of LD iron mats

Iron mats were present at LD every spring and summer throughout our 5-year study period, making them an ideal system for investigating seasonal changes in FeOB mat populations and communities. Following the spring thaw in Maine (between mid-April and early May), LD iron mats first developed in marshy areas at the base of small hummocks and eroded hillsides (Figures 1a and d). The mats were thick (1–3 cm), consolidated, dark in color and overlaid with approximately 1 cm of stagnant or slowly flowing ($<1\,cm\,s^{-1}$) water. By late May and early June, the mats became established in the main stream channels (Figures 1b, c and e). These mats were lighter in color and more flocculent, filling the entire streambed to a depth of 30 cm during 'blooms.'

Systematic microscopic examination of mat samples collected from the marshy areas (Figure 1) in the April of both 2009 and 2010 revealed an abundance of stalk and particulate structures (Figure 2) (indicative of the Gallionellales) and an absence of sheaths. As the mats became established in the main stream channel during May and June, the sheath structures began to dominate (indicative of *Leptothrix spp.*) until stalks or particulates were rare or absent (Figure 2). During the remainder of the summer and through the fall, the sheath structures prevailed until the stream began to freeze (usually mid-November).

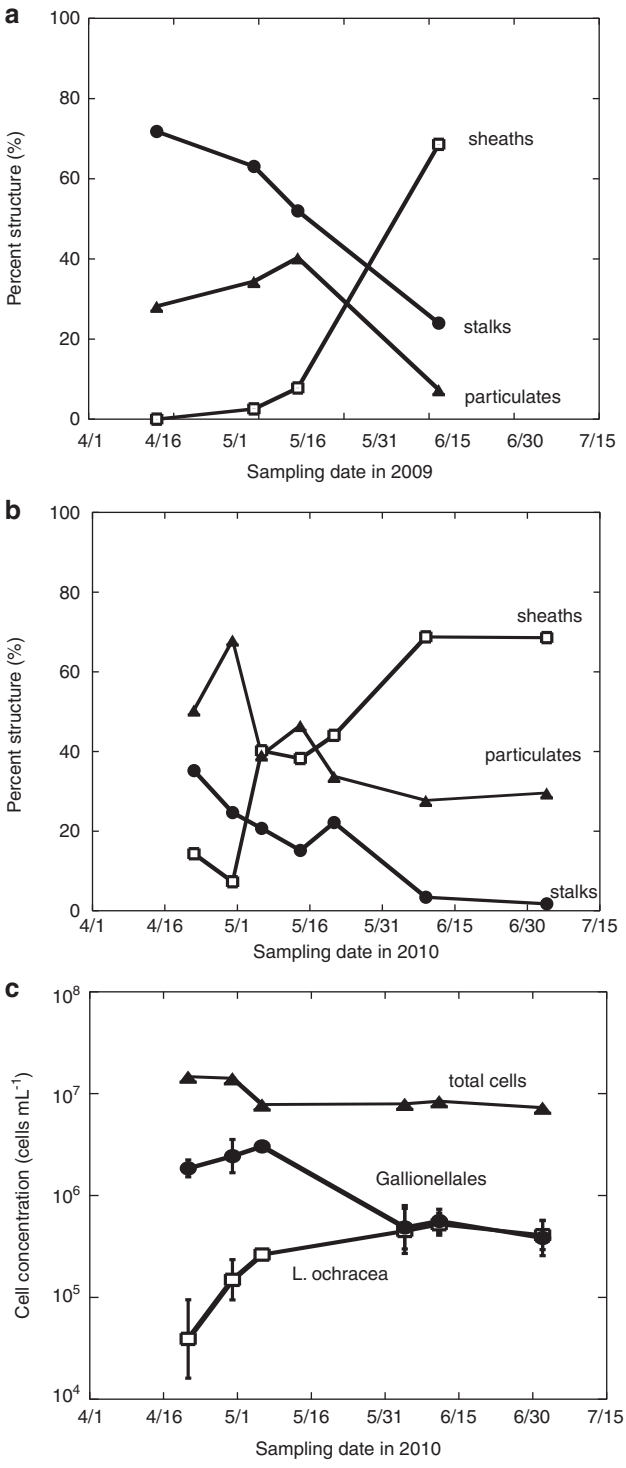

Figure 2. Percent sample containing either sheaths (open squares), stalks (filled circles), or disorganized particulate (triangles) iron-oxyhydroxides in LD during 2009 (**a**) and 2010 (**b**) and concentration of total cells (triangles; cells staining with Syto13), *Gallionellales* cells (filled circles; using FISH probe Gal221) and *L. ochracea* cells (open squares; using Lepto175 probe) (**c**). Error bars represent triplicate samples.

Morphotype and molecular shifts of FeOB in LD iron mats

Water temperatures in LD closely tracked the changes in air temperature, indicating that the stream's primary water source was meteoric rather than a spring-fed system (Supplementary Figure 1). In 2010, relatively few precipitation events occurred in early spring. Intense precipitation events in the late spring/early summer resulted in stream flows $>10\,cm\,s^{-1}$ and completely washed out the flocculent, *Leptothrix*-dominated mats, and in some cases scoured the streambed clean. Following the precipitation events, stream flows and levels decreased within a few days, resulting in a bloom of FeOB and production of new iron mats that were similar in the abundance and type of Fe(III) oxyhydroxide structures prior to the flushing event.

SEM analysis of mats collected in April and June of 2010 not only confirmed light microscopy observations but also revealed the detailed ultrastructure of iron-oxyhydroxide forms (Figure 3). In April, the mats contained all three dominant structural types with stalks being the most abundant morphotype. By June, sheaths dominated; the particulate oxyhydroxides were less dense and formed as clumps on the sheaths. Energy dispersive X-ray analysis confirmed that all structures were composed of iron-oxyhydroxides.

FISH analysis revealed a shift in the prevalent FeOB species at LD (Figure 2). In April and early May of 2010, Gallionellales-related cells dominated the mats, whereas *L. ochracea* cell numbers were not detected. *L. ochracea* cell numbers increased from late May into June and persisted until the end of summer. Lepto175-labeled cells were in chains of 10–50 cells inside a long sheath that was otherwise empty, consistent with the morphology of *L. ochracea*. Some Gal221-labeled cells were bean-shaped and attached to the end of helical stalks, typical of *G. ferruginea*, whereas other Gal221-labeled cells were more rod-shaped, consistent with the morphology of *Sideroxydans* spp., associated with particulate Fe(III)-oxyhydroxides (Weiss *et al.*, 2007). It is important to note that several pure cultures of Gallionellales-related FeOB do not form stalks or identifiable Fe(III)-oxyhydroxide structures (Emerson and Moyer, 1997; Weiss *et al.*, 2007; Lüdecke *et al.*, 2010); thus, the absence of stalks does not necessarily reflect the absence of this FeOB family. This may explain why Gallionellales FISH counts decreased with stalk disappearance but remained present throughout the remainder of the sampling season (Figure 2).

To understand the temporal changes in the microbial community structure of the LD iron mats, the V4–V6 SSU rRNA gene from eight samples (April to September 2010) were pyrotagged, sequenced and compared. The number of high-quality reads recovered varied greatly (471–2340; Table 1), as did the estimated coverage at the 3% similarity clustering level (47.1–96.1%, Table 1). In general, samples collected on 14 May and 21 May were more diverse and had a more even distribution of taxa (lower Berger–Parker indices, greater Inverse Simpson index, Table 1, and greater slope in the rarefaction curves, Supplementary Figure 2). Principal component analysis of community membership produced three different clusters: the 22 April sample, the 14 May sample and the 21 May sample, and the rest of the samples taken later in the

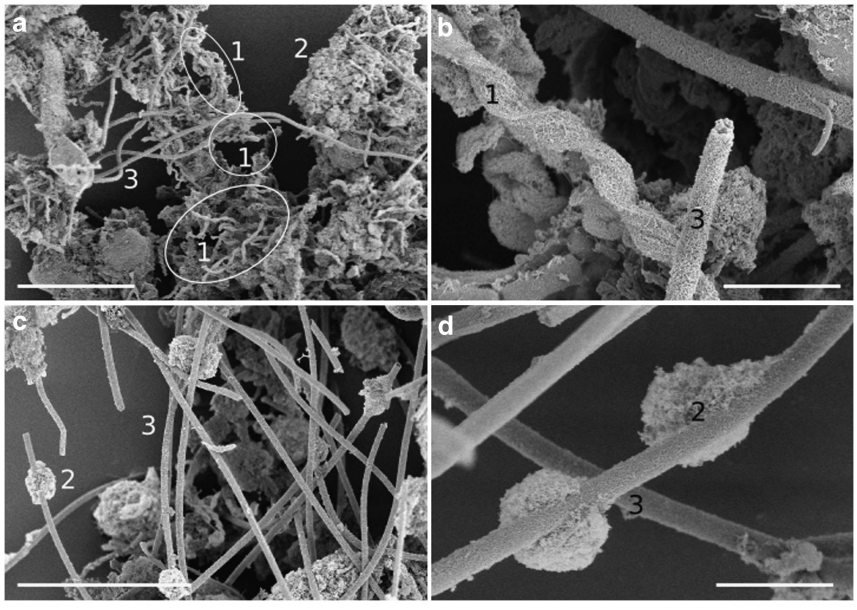

Figure 3 Scanning electron micrographs of mats collected on 22 April (**a, b**) and mats collected on 1 June (**c, d**) with various stalk morphologies (1), disorganized iron-oxyhydroxide particulates (2) and sheaths (3). Scale bars for less magnified images (**a**, **c**) are 30 μm and those for magnified images are 5 μm (**b, d**).

year (Supplementary Figure 5). *Leptothrix* spp. reads increased throughout the season, whereas the Gallionellales reads, after the initial high numbers (sample collected on 22 April), decreased and remained stable (Table 1). The composition of OTUs and total pyrotagged reads also varied over time. The highest OTU-based diversity was encountered in samples collected in mid-May. Samples collected in April or June/July were less diverse, as seen from the higher values of Berger–Parker diversity index (>3). Bacteroidetes reads were most abundant in the Gallionellales-dominated sample collected on 22 April, whereas OTUs associated with various other Betaproteobacteria were abundant in the late summer samples (Supplementary Figure 3). The most abundant OTUs were classified as *Flavobacterium* (in samples collected on 22 April: 24.5% of total pyrotagged reads), unclassified environmental bacteria OTU (1 June: 20.5%; 4 June: 7.0%; 2 July: 12.6%), *Methylobacter* (4 June: 20.0%; 2 July: 17.8%, 30 September: 12.1%) or *Leptothrix ochracea* (4 June: 7.7%, 30 September: 22.4%).

On the basis of these results, the iron mat community can be described as having three phases: a Gallionellales-stalk-dominated phase in April; a relatively rapid transition period in May, with greater overall taxonomic diversity in the mats; and a longer *L. ochracea*-sheath-dominated phase that lasted from late spring through summer/early fall, with less overall diversity compared with the other two phases.

Environmental conditions during iron-mat evolution

Seasonal microbial succession was accompanied with changes in the physicochemical conditions (Table 2). The pH became more acidic with time but stabilized during the transition and *Leptothrix* phases. The denser Gallionellales-dominated mats had steeper oxygen gradients than the flocculent *Leptothrix*-rich mats, and overall oxygen

Table 2 Summary of physicochemical data collected at Lakeside Drive in 2010

Date range in 2010	*Dominant phase*		
	Gallionellales 4/3–5/3	*Transition 5/6–5/23*	*Leptothrix ochracea 5/26–9/30*
Biomarker quantification			
% Stalks	30.0 ± 7.5	19.4 ± 3.7	2.6 ± 1.2
% Sheaths	10.8 ± 5.0	40.8 ± 3.0	68.7 ± 0.1
Physical parameters			
Water temperature (°C)	11.6 ± 1.4	13.1 ± 2.4	15.7 ± 1.4
Rain[a] ($cm\,hr^{-1}$)	0.12 ± 0.18	0.56 ± 0.73	1.0 ± 0.95
Gross chemical parameters			
Change in oxygen with depth from the surface of the mat[b]	$[O_2] = -50(x)\,\mu M\,cm^{-1} + 139\,\mu M$ $R^2 = 0.94$	not determined	$[O_2] = -4(x)\,\mu M\,cm^{-1} + 39\,\mu M$ $R^2 = 0.76$
pH	6.1 ± 0.5	5.2 ± 0.5	5.2 ± 0.2
Dissolved ferrous iron (μM; passed through a filter of 0.2 μm in size)	7 ± 7	59 ± 27	89 ± 70
DOC ($mg\,l^{-1}$)	4.8 ± 1.5	7.3 ± 0.1	7.1 ± 1.3
Spectral slope ratio	1.005 ± 0.021	1.081 ± 0.057	1.128 ± 0.107
Major conservative elemental constituents[c]			
Na	5.26 ± 4.13	0.00 ± 0.00	1.34 ± 1.74
Mg	64.0 ± 32.7	23.4 ± 4.6	57.8 ± 41.1
K	52.4 ± 34.1	26.2 ± 24.6	23.5 ± 20.3
Ca	67.2 ± 21.5	33.1 ± 11.8	53.4 ± 22.4
Cl	126.9 ± 124.1	20.7 ± 1.8	30.0 ± 9.5
Al	3.0 ± 1.0	1.7 ± 0.7	2.8 ± 1.3
Biologically active redox elements[c]			
P	0.3 ± 0.2	1.0 ± 0.9	0.9 ± 0.5
S	55.9 ± 19.3	16.3 ± 5.5	24.4 ± 14.1
Mn	1.6 ± 1.3	2.3 ± 0.9	10.1 ± 10.9
Fe	5.0 ± 4.0	7.3 ± 2.4	22.8 ± 14.4
Ni	0.04 ± 0.02	0.03 ± 0.04	0.009 ± 0.01
Cu	0.6 ± 0.4	1.4 ± 1.7	0.2 ± 0.3
Zn	0.3 ± 0.08	0.7 ± 0.7	0.02 ± 0.1

Abbreviation: DOC, dissolved organic carbon.
[a]Average rain rate during storm.
[b]Where [O2] = oxygen concentration (μM) and x = depth ($\mu M\,cm^{-1}$) into the mat from the surface with ($n = 4$ or 3, respectively).
[c]Elemental concentrations are in μM.

concentrations were significantly higher in the *Leptothrix*-dominated mats (Table 2, Supplementary Figure 4). The DOC concentrations and the spectral slopes ratio increased with time (Supplementary Figure 1), although the averages during each dominant FeOB phase did not differ significantly (Table 2). Similarly, trends in elemental concentration could not easily be assigned to a particular phase of the three-phase model, suggesting a complex system where elemental concentrations might lag or precede changes observed in microbial species (Table 2). Some elements did co-occur with one another, including Fe and Mn ($r^2 = 0.44$, $P = 0.005$) and clay elements Al and Ca ($r^2 = 0.34$, $P = 0.012$) (Supplementary Information 2).

To gain a better understanding of the dynamics and underlying mechanisms controlling the temporal evolution of the community structure at the LD mats, RDA was used to identify trends between population structure and different types of co-registered data (Figure 4). The first two axes of the RDA plots explained a large percentage of the variance in the sample (96.1%) (Figure 4) and reflected relationships discussed previously. For example, *L. ochracea* and Gallionellales are strongly separated along the first axis, a separation that is visible in their respective morphological structures, stalks and sheaths/particulates (Figure 2). The mat development patterns driven by hydrologic changes observed during the past 5 years at LD were apparent in the plot. Gallionellales abundance was located closer to the Al and Ca element vectors, present in clay weathering and groundwater seepage, compared with *L. ochracea* abundance. In contrast, *L. ochracea* was associated with greater rain fall than Gallionellales abundance. This analysis revealed several associations that we had not previously predicted. Species position in the biplot suggests that the transition between two groups of FeOB is reflected in the changes in elemental metal composition, with Gallionellales more often associated with Ni, Cu and Zn, and *L. ochracea* plotting with increased Fe and Mn concentrations. In addition, the RDA identified DOC quantity and size/aromaticity (spectral slope) as an important determinant of *L. ochracea* presence. A second RDA using the same suite of environmental variables (explanatory variables), but with the percentage of tagged pyrosequencing reads assigned to individual species (response variables), gave similar results as the FISH-based RDA (Figure 4).

Discussion

The work presented here shows clear evidence of an ecological succession in biogenic morphotypes of FeOB, from a stalk-dominated (*Gallionella*-related) iron mat ecosystem to one dominated by sheaths (indicative of *L. ochracea*). Molecular analysis shows a concomitant change in microbial population structure, from a predominance of Gallionellales to a greater *L. ochracea* prevalence. This succession was systematically documented for 2 years (2009 and 2010) and was observed each year from 2008 to 2012, indicating that this transition is a cyclic, stable feature of this iron-rich stream ecosystem. The unique iron-oxyhydroxide FeOB morphotypes made it possible to discover and document this succession, giving us the opportunity to resolve the environmental factors driving specific FeOB. Remarkably, the suite of environmental parameters that we measured explained 96% of the variance among the active FeOB (as detected by

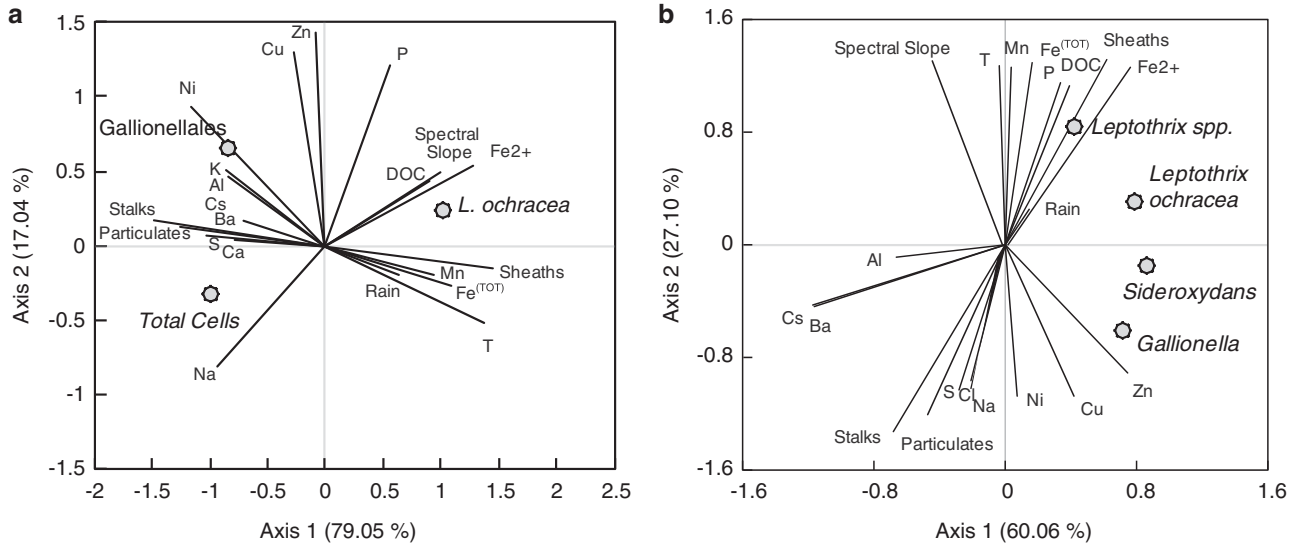

Figure 4. Biplot of RDA of the total cells, total *L. ochracea* cells and Gallionellales cells from direct counts using FISH probes (**a**) or sequence read abundance of specific taxa from pyrosequencing (**b**; dots, response variables) with structural Fe(III)-oxyhydroxide morphotypes, major elements, DOC, air temperature, water temperature and spectral slope of DOC (vectors, explanatory).

FISH) within the surface layer of the LD iron mat ecosystem. This evidence supports the hypothesis for different niche preferences of the two dominant FeOB taxa (Gallionellales and *L. ochracea*), which can explain the ecological succession.

Two mat types prevailed at different positions in the stream, implying the potential role of spatial positioning and associated water flow on community composition. The stalk-forming Gallionellales occurred in condensed mats along seepages associated with the stream banks and weathering-associated elements were greater, and *L. ochracea* developed in deeper, free-flowing stream sections and during greater rainfall. Other studies have observed *L. ochracea* growing in condensed mats with greater water flows (Emerson and Revsbech, 1994) and the presence of Gallionellales populations in slow-moving water channels (Harder, 1919; Rentz *et al.*, 2007; Emerson unpublished observations). Hydrologic flow regimes are important determinants in chemical lability and mixing, and thus may help drive the differential spatial positioning of seasonal FeOB mats. For example, evidence suggests that Gallionellales are restricted to more oxygen-depleted habitats, and *L. ochracea* has a wider tolerance of oxygen concentrations (Emerson and Revsbech, 1994; Rentz *et al.*, 2007), although exceptions have been reported in *L. ochracea* mats with little O_2 penetration (Emerson and Revsbech, 1994; Roden *et al.*, 2012) and in technical water systems where stalk-forming Gallionella were present at high O_2 concentrations (Søgaard *et al.*, 2001; de Vet *et al.*, 2011). Nonetheless, this hypothesis is consistent with oxygen profiles at LD: mats dominated by Gallionellales had steep oxygen gradients, and *L. ochracea* mats had more gradual oxygen gradients with overall oxygen concentrations that approached half-saturation.

It is plausible that synergistic effects of hydrodynamics, temperature, metal concentration and oxygen in LD create conditions favorable for a succession in FeOB dominance. Other studies on FeOB communities (both neutrophilic and acidophilic) have observed general changes in community structure that correspond with temperature, season or rain (Edwards *et al.*, 1999; Hegler *et al.*, 2012; Johnson *et al.*, 2012). In particular, Gault *et al.* (2012) sampled a spring-fed iron mat in Chalk River, Ontario, once during each major season, and noted that the abundance of Gallionellales clones was greater in winter than in summer, consistent with the findings presented here. Interestingly, they also noted that sheaths were the dominant morphotype present throughout the year at this site, although conventional SSU rRNA clone libraries did not reveal the presence of *L. ochracea*. Seasonal temperature change may also be a proxy for other factors that are changing and altering population dynamics, rather than these changes being solely due to the specific temperature sensitivity of a population. Other variables including DOC concentration, size and aromaticity may also be an important determinant of population structure of specific FeOB taxa, particularly for *L. ochracea* populations (Figure 4). The cause of the seasonal shifts in the spectral slope ratio might be indicative of change in the dissolved matter origin, or due to different photochemical, biological or aggregation processes that are known to alter DOC MW and aromaticity (Floge and Wells, 2007; Helms *et al.*, 2008). These findings as applied to the LD system could indicate the following: (1) Steep increases in spectral ratio associated with rain events bring in un-degraded organic material—compared with the ratios associated with older decomposed detrital matter of stagnant waters—as a fresh source of organic matter that provides a fresh carbon source (Chow *et al.*, 2013). (2) The increase in rain-associated cloud cover causes a decrease in DOC photobleaching, the sunlight-induced conversion of larger, aromatic DOC molecules (larger spectral slope) into smaller MW molecules (smaller spectral slope), as demonstrated by Helms *et al.* (2008). Either possibility exposes a previously unexplored relationship between *L. ochracea* and organic carbon cycling.

Bogs, fens, tile drains and certain chalybeate springs are typically organic-rich environments and can be abundant with *L. ochracea*-rich mats (Harder, 1919). These waters, rich in complex decaying organic matter, retain Fe(II) and Fe(III) in solution despite circum-neutral pH or oxygenation (Emmenegger *et al.*, 1998; Dhungana and Crumbliss 2005). *L. ochracea* seems to have an absolute requirement for high concentrations of iron (van Veen *et al.*, 1978; Ghiorse, 1984; Emerson *et al.*, 2010; Fleming, unpublished results), yet tolerates and proliferates in oxygen-rich environments, as demonstrated at LD. To exploit such niches, *L. ochracea* would require retardation of abiotic iron oxidation. By changing the iron reaction rates and retaining iron in solution, organic ligands (Liang *et al.*, 1993; Rose and Waite, 2003) may promote *L. ochracea* growth. Alternatively the co-occurrence of *L. ochracea* and DOC may indicate that *L. ochracea* requires the DOC to grow heterotrophically or mixotrophically. Assimilation of carbon by *L. ochracea* has been debated for the past century (van Veen *et al.*, 1978; Ghiorse, 1984; Winogradsky, 1888). The argument for heterotrophy relies on *L. ochracea's* close phylogenetic affiliation with heterotrophic relatives. Conversely, the arguments for autotrophy are based on its growth and ecological preferences, such as the production of small volumes of biomass with the need for high amounts of Fe(II) (a low-yielding energy source), and on its inability to grow on heterotrophic media (Emerson *et al.*, 2010). Preliminary data suggest that *L. ochracea* contains genes for carbon fixation (Fleming *et al.*, unpublished results).

The physiology and ecology of Gallionellales is better understood, in part because cultured representatives are available. These representatives

include chemolithoautotrophs, which generate either stalks or particulate iron-oxyhydroxides and typically require low oxygen tensions (Emerson and Revsbech, 1994; Druschel *et al.*, 2008; Li *et al.*, 2010). The Gallionellales are phylogenetically diverse with several cultivated genera (reviewed in Emerson *et al.*, 2010; Lüdecke *et al.*, 2010; Krepski *et al.*, 2011); Gallionellales SSU rRNA sequences are consistently abundant in clone libraries from iron mats (Haaijer *et al.*, 2008; Duckworth *et al.*, 2009; Wang *et al.*, 2009; Bruun *et al.*, 2010; Fleming *et al.*, 2011; Gault *et al.*, 2012; Kato *et al.*, 2012; Roden *et al.*, 2012). In April, LD iron mats began forming at localized seepage sites. Gallionellales stalks, cells and sequences were abundant, the oxygen gradients were steepest and the pH was greater. The RDA indicated that Gallionellales and stalk abundance negatively co-occurred with high concentrations of total iron, Mn, organic carbon complexity (spectral slope) and DOC. Then in May, when stalks and total Gallionellales cell counts decreased with time, the percentage of Gallionellales cells to total cells did not fall below 5% of the total population during the sampling period. In a second RDA with environmental variables and classified tagged pyrosequencing read abundance (Figure 4), *Gallionella* spp. coincided with stalks and particulates more often than did sheaths, and *Sideroxydans* spp. (not known to produce organized extracellular structures) did not coincide with any particular structure. These data indicate the presence of at least two Gallionellales populations in these mats, and that may change their physiology in response to seasonal signals. First, there is a stalk-forming Gallionellales population that prefers environments with tightly constrained redoxclines, environments in which Fe(II) is not stabilized by organic carbon and lower pH and thus Fe(II) does not persist in the more oxygenated zones above the mat. Second, there is a non-stalk-forming Gallionellales population that does not have a seasonal preference; possibly these cells adhere to the sheaths or stalks produced by other FeOB, to maintain an optimum position to access both iron and oxygen. A population succession among Gallionellales may explain why even in sheath-rich iron mats there are so many Gallionellales–SSU rRNA sequences present.

Several other taxa were consistently recovered at high percentages in the pyrotagged reads, including specific members of Bacteriodetes and presumptive methylotrophs. For example, *Flavobacterium* reads (24.5%) were evident in the Gallionellales-dominated April sample after the stalk-sheath transition (late May) *Methylobacter* (5.8–20% of total sequences) and unidentified environmental OTUs (6.5–20.5%) were conspicuous in the *L. ochracea*-dominated samples. Sequences from these same taxa were recovered from multiple other neutrophilic iron mats, and there is growing evidence of the co-occurrence of OTUs related to *Methylobacter* or *Flavobacterium* with either *L. ochracea* or Gallionellales (Bruun *et al.*, 2010; Fru *et al.*, 2012; Johnson *et al.*, 2012; Kato *et al.*, 2012). Recent work has more rigorously established linkages among taxa and functional genes related to methanotrophs or methylotrophs being present in iron-oxidizing ecosystems (Wang *et al.*, 2012; Kato *et al.*, 2013). It is not clear why these taxa regularly occur in high Fe(II) environments associated with FeOB. Although the capacity of some of these taxa to use Fe(II) as an energy source cannot be ruled out, it is more likely that redoxcline habitats where Fe(II) is abundant also contain methane. The interesting question will be to determine whether there are specific co-occurrences of these groups, which could suggest some type of mutualism, commensalism, competitive co-existence or niche overlap.

The present work reveals that it is likely a complex interplay of physical and chemical factors that results in a marked ecological succession between the Gallionellales and *L. ochracea*. Further work is required to determine which factor or factors, for example quantity and quality of DOC, might provide a tipping point that drives dominance of one group within the microbial mat community. Because iron mats are easily recognized by the eye, and the characteristic stalks or sheaths are easily recognized by light microscopy, FeOB provide a useful model for studying the role of physiological adaptations and behavioral strategies in ecological succession and competition.

Conflict of Interest

The authors declare no conflict of interest.

Acknowledgements

We would like to thank Steve Bryer and David Gaecklin for regular access to the LD field site, Carly Hallowell for processing the ICP-OES data, Debbie Powell for SEM analyses, and Prof. Mary Jane Perry for support and discussion. We are also grateful to Dr Joyce McBeth, Nicole Brisson, Dr Beth Orcutt, Dr Jarrod J. Scott and Jaime Blair for help with data collection, data processing and comments on the manuscript. This work was funded by support from the National Science Foundation (IOS-0951077). IC would like to acknowledge the support from NASA (NNX13AC42G).

Author contributions

EJF—designing, analysis, writing; IC—analysis, instrumentation, writing; CSC—analysis, instrumentation, writing; DWK—analysis, instrumentation; DE—designing, analysis, writing.

References

Bruun A-M, Finster K, Gunnlaugsson H, Nørnberg P, Friedrich MW. (2010). A comprehensive investigation of iron cycling in a freshwater seep including microscopy, cultivation and molecular community analysis. *Geomicrobiol J* **27**: 15–34.

Chan CS, Fakra SC, Emerson D, Fleming EJ, Edwards KJ. (2011). Lithotrophic iron-oxidizing bacteria produce organic stalks to control mineral growth: implications for biosignature formation. *ISME J* **5**: 717–727.

Chow AT, Dai J, Conner WH, Hitchcock DR, Wang J-J. (2013). Dissolved organic matter and nutrient dynamics of a coastal freshwater forested wetland in Winyah Bay, South Carolina. *Biogeochem* **112**: 571–587.

de Vet WWJM, Dinkla IJT, Rietveld LC, van Loosdrecht MCM. (2011). Biological iron oxidation by *Gallionella* spp. in drinking water production under fully aerated conditions. *Water Res* **45**: 5389–5398.

Dhungana S, Crumbliss A. (2005). Coordination chemistry and redox processes in siderophore-mediated iron transport. *Geomicrobiol J* **22**: 87–98.

Dowd SE, Callaway TR, Wolcott RD, Sun Y, McKeehan T, Hagevoort RG *et al.* (2008). Evaluation of the bacterial diversity in the feces of cattle using 16S rDNA bacterial tag-encoded FLX amplicon pyrosequencing (bTEFAP). *BMC Microbiol* **8**: 125.

Druschel G, Emerson D, Sutka R, Suchecki P, Luther GW III. (2008). Low-oxygen and chemical kinetic constraints on the geochemical niche of neutrophilic iron(II) oxidizing microorganisms. *Geochim Cosmochim Acta* **72**: 3358–3370.

Duckworth OW, Holmstrom S, Pena J, Sposito G. (2009). Biogeochemistry of iron oxidation in a circumneutral freshwater habitat. *Chem Geol* **260**: 149–158.

Edwards KJ, Gihring TM, Banfield JF. (1999). Seasonal variations in microbial populations and environmental conditions in an extreme acid mine drainage environment. *Appl Environ Microbiol* **65**: 3627–3632.

Emerson D, Fleming EJ, McBeth JM. (2010). Iron-oxidizing bacteria: an environmental and genomic perspective. *Annu Rev Microbiol* **64**: 561–583.

Emerson D, Weiss J. (2004). Bacterial iron oxidation in circumneutral freshwater habitats: findings from the field and the laboratory. *Geomicrobiol J* **21**: 405–414.

Emerson D, Moyer CL. (1997). Isolation and characterization of novel iron-oxidizing bacteria that grow at circumneutral pH. *Appl Environ Microbiol* **63**: 4784–4792.

Emerson D, Moyer CL. (2002). Neutrophilic Fe-oxidizing bacteria are abundant at the Loihi Seamount hydrothermal vents and play a major role in Fe oxide deposition. *Appl Environ Microbiol* **68**: 3085–3093.

Emerson D, Revsbech N. (1994). Investigation of an iron-oxidizing microbial mat community located near Aarhus, Denmark: field studies. *Appl Environ Microbiol* **60**: 4022–4031.

Emmenegger L, King D, Sigg L, Sulzberger. B. (1998). Oxidation kinetics of Fe (II) in a eutrophic Swiss lake. *Environ Sci Technol* **32**: 2990–2996.

Fleming EJ, Langdon AE, Martinez-Garcia M, Stepanauskas R, Poulton NJ, Masland EDP *et al.* (2011). What's new is old: resolving the identity of *Leptothrix ochracea* using single cell genomics, pyrosequencing and FISH. *PLoS One* **6**: e17769.

Floge SA, Wells ML. (2007). Variation in colloidal chromophoric dissolved organic matter in the Damariscotta Estuary, Maine. *Limnol and Oceanogr* **52**: 32–45.

Fru EC, Piccinelli P, Fortin D. (2012). Insights into the global microbial community structure associated with iron oxyhydroxide minerals deposited in the aerobic biogeosphere. *Geomicrobiol J* **29**: 587–610.

Fuchs BM, Pernthaler J, Amann R. (2007). Single cell identification by fluorescence *in situ* hybridization Beveridge TJ, Reddy CA, Breznak JA, Marzluf G, Schmidt TM, Snyder LR (eds). *Methods Gen Mol Microbiol*. ASM press: Washington DC, pp 886–896.

Gault AG, Langley S, Ibrahim A, Renaud R, Takahashi Y, Boothman C *et al.* (2012). Seasonal changes in mineralogy, geochemistry and microbial community of bacteriogenic iron oxides (BIOS) deposited in a circumneutral wetland. *Geomicrobiol J* **29**: 161–172.

Ghiorse W. (1984). Biology of iron- and manganese-depositing bacteria. *Annu Rev Microbiol* **38**: 515–550.

Haaijer SCM, Harhangi HR, Meijerink BB, Strous M, Pol A, Smolders AJP *et al.* (2008). Bacteria associated with iron seeps in a sulfur-rich, neutral pH, freshwater ecosystem. *ISME J* **2**: 1231–1242.

Harder E. (1919). *Iron-depositing bacteria and their geologic relations*. Department of the Interior, Government Printing Office: Washington DC.

Hegler F, Lösekann-Behrens T, Hanselmann K, Behrens S, Kappler A. (2012). Influence of seasonal and geochemical changes on the geomicrobiology of an iron carbonate mineral water spring. *Appl Environ Microbiol* **78**: 7185–7196.

Helms JR, Stubbins A, Ritchie JD, Minor EC, Kieber DJ, Mopper K. (2008). Absorption spectral slopes and slope ratios as indicators of molecular weight, source, and photobleaching of chromophoric dissolved organic matter. *Limnol and Oceanogr* **53**: 955–969.

Johnson KW, Carmichael MJ, McDonald W, Rose N, Pitchford J, Windelspecht M *et al.* (2012). Increased abundance of *Gallionella* spp., *Leptothrix* spp. and total bacteria in response to enhanced Mn and Fe concentrations in a disturbed southern Appalachian high elevation wetland. *Geomicrobiol J* **29**: 124–138.

Kato S, Kikuchi S, Kashiwabara T, Takahashi Y, Suzuki K, Itoh T *et al.* (2012). Prokaryotic abundance and community composition in a freshwater iron-rich microbial mat at circumneutral pH. *Geomicrobiol J* **29**: 896–905.

Kato S, Chan C, Itoh T, Ohkuma M. (2013). Functional gene analysis of freshwater iron-rich flocs at circumneutral pH and isolation of a stalk-forming microaerophilic iron-oxidizing bacterium. *Appl Environ Microbiol* **79**: 5283–5290. (Early Release).

Kent AD, Yannarell AC, Rusak JA, Triplett EW, McMahon KD. (2007). Synchrony in aquatic microbial community dynamics. *ISME J* **1**: 38–47.

Katsoyiannis IA, Zouboulis AI. (2006). Use of iron- and manganese-oxidizing bacteria for the combined removal of iron, manganese and arsenic from contaminated groundwater. *Water Qual Res J Can* **41**: 117–129.

Krepski ST, Hanson TE, Chan CS. (2011). Isolation and characterization of a novel biomineral stalk-forming iron-oxidizing bacterium from a circumneutral groundwater seep. *Environ Microbiol* **14**: 1671–1680.

Liang L, McNabb JA, Paulk JM, Gu B, McCarthy JF. (1993). Kinetics of Fe(II) oxygenation at low partial pressure of oxygen in the presence of natural organic matter. *Environ Sci Tech* **27**: 1864–1870.

Li D, Li Z, Yu J, Cao N, Liu R, Yang M. (2010). Characterization of bacterial community structure in a drinking water

distribution system during an occurrence of red water. *Appl Environ Microbiol* **76**: 7171–7180.
Lüdecke C, Reiche M, Eusterhues K, Nietzsche S, Küsel K. (2010). Acid-tolerant microaerophilic Fe(II)-oxidizing bacteria promote Fe(III)-accumulation in a fen. *Environ Microbiol* **12**: 2814–2825.
Ludwig W, Strunk O, Westram R, Richter L, Meier H, Yadhukumar *et al.* (2004). ARB: a software environment for sequence data. *Nucleic Acids Res* **32**: 1363–1371.
McBeth JM, Fleming EJ, Emerson D. (2013). The transition from freshwater to marine iron-oxidizing bacterial lineages along a salinity gradient on the Sheepscot River, Maine USA. *Environ Microbiol Rep* **5**: 453–463.
Pruesse E, Quast C, Knittel K, Fuchs BM, Ludwig W, Peplies J *et al.* (2007). SILVA a comprehensive online resource for quality checked and aligned ribosomal RNA sequence data compatible with ARB. *Nucleic Acids Res* **35**: 7188–7196.
R Core Team (2012). *R: A Language and Environment for Statistical Computing*. R Foundation for Statistical Computing: Vienna, Austria, ISBN 3-900051-07-0http://www.R-project.org/.
Ramette A. (2007). Multivariate analyses in microbial ecology. *FEMS Microbiol Ecol* **62**: 142–160.
Rasband W. (2004). ImageJ: image processing and analysis in java. Book Public Domain, http://rsbweb.nih.gov/ij/.
Rentz JA, Kraiya C, Luther GW III, Emerson D. (2007). Control of ferrous iron oxidation within circumneutral microbial iron mats by cellular activity and autocatalysis. *Environ Sci Technol* **41**: 6084–6089.
Roden EE, McBeth JM, Blöthe M, Percak-Dennett EM, Fleming EJ, Holyoke RR *et al.* (2012). The microbial ferrous wheel in a neutral pH groundwater seep. *Front Microbiol* **3**: 172.
Rose A, Waite T. (2003). Effect of dissolved natural organic matter on the kinetics of ferrous iron oxygenation in seawater. *Environ Sci Technol* **37**: 4877–4886.
Schloss PD, Gevers D, Westcott SL. (2011). Reducing the effects of PCR amplification and sequencing artifacts on 16S rRNA-based studies. *PLoS One* **6**: e27310.
Søgaard EG, Aruna R, Abraham-Peskir J, Koch CB. (2001). Conditions for biological precipitation of iron by *Gallionella ferruginea* in a slightly polluted ground water. *Appl Geochem* **16**: 1129–1137.
Stookey LL. (1970). Ferrozine—a new spectrophotometric reagent for iron. *Anal Chem* **42**: 779–781.
Sugimura Y, Suzuki Y. (1988). A high temperature catalytic oxidation method for the determination of non-volatile dissolved organic carbon in seawater by direct injection of a liquid sample. *Mar Chem* **24**: 105–131. (EPA Method 415.1).
van Veen W, Mulder E, Deinema M. (1978). The *Sphaerotilus-Leptothrix* group of bacteria. *Microbiol Rev* **42**: 329–356.
Wang J, Muyzer G, Bodelier PLE, Laanbroek HJ. (2009). Diversity of iron oxidizers in wetland soils revealed by novel 16S rRNA primers targeting *Gallionella*-related bacteria. *ISME J* **3**: 715–725.
Wang J, Krause S, Muyzer G, Meima-Franke M, Laanbroek HJ, Bodelier PLE. (2012). Spatial patterns of iron- and methane-oxidizing bacterial communities in an irregularly flooded, riparian wetland. *Front Microbiol* **3**: 1–13.
Weiss JV, Rentz JA, Plaia T, Neubauer SC, Merrill-Floyd M, Lilburn T *et al.* (2007). Characterization of neutrophilic Fe(II)-oxidizing bacteria isolated from the rhizosphere of wetland plants and description of *Ferritrophicum radicicola* gen. nov. sp. nov., and *Sideroxydans paludicola* sp. nov. *Geomicrobiol J* **24**: 559–570.
Winogradsky S. (1888). Ueber Eisenbacterien. *Botanishe Zeitung* **46**: 261–271.

Supplementary Information accompanies this paper on The ISME Journal website (http://www.nature.com/ismej)